



We are Nitinol.™

**Two-Step Martensitic Transformations in TiNi (10% Cu) Shape Memory Alloy**

Moberly, Duerig, Proft, Sinclair

Materials Research Society Symposium Proceedings Vol. 245  
"Shape Memory Materials and Phenomena - Fundamental Aspects and Applications"  
pp. 55-60

1992

## TWO - STEP MARTENSITIC TRANSFORMATIONS IN TiNi(10% Cu) SHAPE MEMORY ALLOYS

WARREN J. MOBERLY\*, T.W. DUERIG\*\*, J.L. PROFT\*\* AND R. SINCLAIR\*\*\*

\* Dept. of Materials Science & Engineering, Stevens Institute of Technology, Hoboken, NJ

\*\* Raychem Corporation, Menlo Park, CA

\*\*\* Dept. Materials Science & Engineering, Stanford University, Stanford, CA

### ABSTRACT

Third element additions to TiNi provide a wide range of modifications of its shape memory properties. The advantages of Cu additions are to provide a more narrow hysteresis, less sensitivity to the Ti:Ni(+Cu) ratio of the temperature at which martensite starts to form ( $M_S$ ), a larger strength differential between the austenite and martensite phases, and superior fatigue resistance. The substitution of a few atomic percent Cu for Ni does not significantly alter the crystal structure of either the cubic B2 austenite nor the monoclinic B19' martensite phases; however, the addition of greater than 10% Cu results in an orthorhombic B19 martensite phase. For the case of 10% Cu, a two-step martensitic transformation occurs upon cooling, with the cubic austenite transforming to the orthorhombic B19 martensite and subsequently to the monoclinic B19' martensite. As a result of this two-step crystallographic transformation, material properties such as resistivity and shape change also exhibit a two-step transformation.

*In situ* transmission electron microscopy heating and cooling experiments are used to observe the two-step martensitic transformation and to establish an orientation relationship between the B19 orthorhombic and the B19' monoclinic structures. Strain vs temperature  $M_S$  tests establish the relative shape changes associated with both the cubic-to-orthorhombic transformation and the orthorhombic-to-monoclinic transformation. Similar  $M_S$  tests, where an applied load is removed during the transformation, establishes a crystallographic dependence between the two shape changes. Whereas binary TiNi is "trained" to undergo a specific shape change, this ternary TiNiCu alloy has a "natural" direction associated with the second step of its shape change.

### INTRODUCTION

As Shape Memory Materials develop from an interesting materials phenomena to products with useful engineering applications, control and modification of the shape memory properties become important. In the case of TiNi alloys, one particularly important parameter, the martensitic transformation temperature ( $M_S$ ), can be modified by the addition of ternary alloying elements. A second parameter, the extent of shape change realized, can be modified when the ternary addition(s) is sufficient to cause a change in the crystal structure(s) of the martensite and/or austenite phases. Typically only small concentrations (1-2%) of ternary elements are possible without the formation of second phases that are detrimental to the shape memory effect.

Ternary  $Ti_{50}Ni_{(50-x)}Cu_x$  alloys provide a number of useful modifications to the martensitic transformation and consequently the shape memory effect, while allowing for the substitution of >20% Cu for Ni. The addition of Cu results in a more narrow hysteresis between the temperatures of the austenite-to-martensite and reverse martensite-to-austenite transformations [1, 2, 3]. Such a narrow hysteresis has the advantage of causing a "quicker" shape change, requiring a smaller deviation during thermal cycling. Whereas the  $M_S$  temperature of binary TiNi alloys drops dramatically due to minor increases in the Ni:Ti ratio, the addition of Cu makes the  $M_S$  temperature less sensitive to this ratio [4]. Thus ternary TiNiCu shape memory parts are less subject to concentration variations that are present in bulk processed materials.

Although an early study [5] of ternary TiNiCu alloys indicated the martensitic phase had a monoclinic structure even for concentrations of copper greater than 20%, more recent studies have determined that the equilibrium phase for higher Cu-containing alloys (>15% Cu) has an

orthorhombic structure [2, 6, 7, 8]. (Depending on processing conditions either the orthorhombic or monoclinic martensites are possible for ternary alloys comprised of ~15% to 25% Cu [1].) The substitution of greater than 25% Cu for Ni had been observed in the high temperature austenite phase without having significantly altered the 0.302 nm lattice parameter of the B2 cubic phase [4, 9]. The low temperature phase, the monoclinic martensite which formed for Cu concentrations below 10% [2, 5, 6, 7, 8], exhibited the same lattice parameters ( $a_0 = 0.289$ ,  $b_0 = 0.462$ , and  $c_0 = 0.412$  nm) as that of the binary TiNi alloy [10]. However, a Cu concentration >15% resulted in a slight modification of lattice parameters ( $a_0 = 0.289$ ,  $b_0 = 0.451$ , and  $c_0 = 0.4265$  nm), as well as a change in angle to form the orthorhombic lattice [2, 8]. For intermediate copper concentrations (~10%), both the orthorhombic and monoclinic phases have been observed at successive temperatures [7], where the orthorhombic structure existed as an intermediate step in the distortion when transforming from cubic to monoclinic.

Not only did the ternary TiNiCu alloys exhibit a different martensitic crystal structure, as compared to the binary TiNi alloy, they also exhibited different twinning systems within the martensite grains. Three distinct twinning planes have been observed in monoclinic B19' martensite of binary TiNi alloys: (111) [11], (011) [12], and (010) [13], with the (111) twinning being predominant. The smaller distortion involved in the cubic-to-orthorhombic martensitic transformation of TiNiCu alloys (with >15% Cu) resulted in (011) twinning being the dominant twinning system [2]. In addition, the (010) twin plane did not exist for the orthorhombic martensitic structure of these ternary alloys. Instead some grains of the orthorhombic martensite exhibited a twinless microstructure [2, 8]. The crystallographic relationships existing for the cubic-to-monoclinic martensitic transformation of the binary alloy were determined to be similar to those of the cubic-to-orthorhombic transformation in ternary alloys. A general {hkl} plane in the cubic B2 structure became the same {h'k'l'} plane in the martensite, independent of whether the martensite was monoclinic or orthorhombic. For both transformations, the matrix relationships to form ( $\bar{1}11$ ) and (011) twins had the same relative multiplicity, with the formation of 24 variants of martensite being possible. The crystallographic relationship between the orthorhombic and monoclinic structures was determined to be limited such that only two variants would form during the orthorhombic-to-monoclinic martensitic transformation. (This limited crystallographic relationship in turn dictates the two-step shape memory change discussed in this study.) In an earlier study it was suggested that *in situ* TEM observation of the transformation from twinned orthorhombic martensite to twinned monoclinic martensite would establish the relative distortion of the two successive shape changes.

## EXPERIMENTAL PROCEDURES

In conjunction with a previous study [2, 8] TiNiCu alloys were prepared from high purity (99.99%) metals by vacuum plasma-melting and casting one kilogram ingots. Alloys of different compositions, with Cu ranging from 0% to 25%, were used as a basis to determine the different crystal structures and microstructures possible. The as cast and annealed materials were evaluated using x-ray diffraction, x-ray fluorescence, scanning electron microscopy, energy dispersive x-ray spectroscopy, differential scanning calorimetry, transmission electron microscopy, and *in situ* heating and cooling TEM experiments [8]. In this study the ternary alloy with 10% Cu was further processed by extrusion and drawing to form wires of 3 mm and 0.45 mm diameters. After drawing, these wires were reannealed at 750°C for 2 hours.

Optical microscopy determined that the typical grain size was 10 - 40  $\mu\text{m}$  and that primarily one phase existed. (Oxide precipitates constituted less than 1 vol.% of the microstructure and therefore have minor effect on the martensitic transformation.) The wires of 3 mm diameter were sliced into discs ~0.5 mm in thickness. TEM samples were prepared by grinding these discs to a thickness of ~0.07 mm followed by electropolishing in an electrolyte of 75 vol.% methanol and 25 vol.% nitric acid at -20°C and 12 volts [14]. TEM (with Philips EM400 and EM430 microscopes) was used to evaluate the microstructure, crystal structure, and types of twins present in the martensitic phases. *In situ* heating and cooling experiments were used to observe the two-step martensitic transformation.

The wires of 0.45 mm diameter were subjected to thermal cycling while having a load applied. The wire was first heated to a fully austenitic condition, and then a constant load was applied. Subsequent thermal cycling was performed by flowing cooled nitrogen gas over the wire to cool below -70°C, followed by convective heating with nitrogen gas to above 70°C.

Measuring the elongation of the wire as a function of temperature established the start and finish of both the austenite-to-martensite and reverse martensite-to-austenite phase transformations. These strain vs temperature " $M_S$  tests" were used to evaluate the relative strain that would be realized in a shape memory application. For these 10% Cu ternary alloys, these  $M_S$  tests established the presence of a two-step shape change arising due to the two-step martensitic transformation. The  $M_S$  temperature in a strain vs temperature test increases as a function of the applied load [2, 15, 16]. A previous study had determined that applied loads in excess of 150 MPa resulted in the loss of the two step shape change, as the  $M_S$  of the stress-induced transformation to monoclinic martensite was raised to a temperature above that of the  $M_S$  temperature of the cubic-to-orthorhombic transformation [2, 17]. Thus for this study the applied load was kept at 60 MPa. A series of strain vs temperature  $M_S$  tests were conducted on an annealed wire. (It is noted that wires with vestiges of cold worked microstructures will exhibit "training" which influences the elongation realized in these  $M_S$  tests. An annealed wire, however, will exhibit no shape change if no load is applied during a  $M_S$  test.) In order to evaluate the relative strains in each of the two successive transformations, sequential  $M_S$  tests were conducted where the load was removed during different stages of the martensitic transformations.

## EXPERIMENTAL RESULTS

A more complete evaluation of the microstructure of TiNiCu alloys, as a function of copper concentration has been presented in other published works [2, 8, 18]. The microstructures observed in these previous studies have also been discussed in light of their relation to microstructure evaluations presented by other research groups [5, 6]. All TEM samples prepared from the  $Ti_{50}Ni_{40}Cu_{10}$  alloy exhibited the B19' monoclinic martensite phase at room temperature. As noted in a previous study [8], the major type of twinning was (111), however with (010) twinning being more prevalent than has been typically observed for the binary TiNi alloy. The (111) twins were often observed to be >100 nm in width, and the (010) twins were typically tens of nanometers in width. In this previous study *in situ* TEM heating experiments had realized only the transformation directly from monoclinic B19' martensite to the cubic B2 austenite, and subsequent cooling had resulted in only the reverse transformation, with the orthorhombic martensite phase never being realized in the 10% Cu ternary alloy. (It is also noted that *in situ* TEM heating and cooling experiments often exhibit  $A_S$  and  $M_S$  temperatures that are higher and lower, respectively, than observed during DSC measurements of "bulk" samples. Such anomalies in phase transformations in thin films have commonly been observed in other studies of TiNi alloys.) However, repeated experiments in this present study did result in the formation of the orthorhombic martensite from the cubic austenite upon cooling.

After heating the TEM sample inside the microscope to form the B2 structure, subsequent slow cooling resulted in the observation of the transformation to the B19 structure. The orthorhombic martensite exhibited (111) twinning, with the fine spacing of <30 nm presumably due to thin foil effects of the TEM sample. Upon subsequent cooling to -100°C, even finer twins (3-4 nm in width and exhibiting the (010) twin plane) of monoclinic martensite formed within the orthorhombic twins. Upon subsequent heating these (010) twins disappeared as the monoclinic martensite transformed back to the orthorhombic martensite. This transformation was evident in the BF TEM images acquired at -51°C and -37°C and presented in Figures 1b and 1c, respectively. This monoclinic-to-orthorhombic transformation was confirmed by the disappearance of streaking and the change in angle between (010) and (101) g-vectors in [101] zone axis selected area electron diffraction patterns acquired at -59°C and -34°C and presented in Figures 1a and 1d, respectively.

The series of  $M_S$  tests, with the 60 MPa load being removed at progressive stages of the martensitic transformation, have been presented in Figures 2a through 2e. The strain vs temperature curve of Figure 2a was a standard, where the load was applied throughout the test. As had been previously observed for this TiNi(10% Cu) shape memory alloy, a two-step shape change occurred. Upon cooling, the cubic austenite-to-orthorhombic martensite transformation started at ~25°C and the subsequent orthorhombic martensite-to-monoclinic martensite transformation started at -12°C. The reverse transformations upon heating started at -10°C and 35°C for the monoclinic-to-orthorhombic and orthorhombic-to-cubic transformations, respectively. For the tests where the load was removed, these reverse transformations started at slightly higher temperatures of -20°C and 30°C, respectively.

When the load was first applied to the wire in the austenitic condition, an elastic strain of 0.4% occurred without any stress-induced martensite being formed. This same elastic strain was observed during loading for each of the  $M_S$  tests. After thermal cycling in the plot of Figure 2a, the removal of the applied load resulted in the recovery of all of the elastic strain. For Figures 2b through 2e the elastic strain was recovered when the load was removed during the  $M_S$  test. However, the strain recovered in each of these unloading conditions was 0.6%, implying more than elastic strain was recovered during unloading.

The pseudoelastic strain (i.e. strain associated with the shape memory effect) was separated into two components. For the standard test of Figure 2a, a strain of 2.25% was achieved during the cubic-to-orthorhombic transformation, and a strain of 1% occurred during the subsequent orthorhombic-to-monoclinic transformation. (As presented in previous studies [1, 8, 17], a greater strain is possible with a higher applied load and/or "training".) For the  $M_S$  test in Figure 2b the load was removed just before the beginning of the second (orthorhombic-to-monoclinic) transformation. Even though no load was applied as the sample was further cooled, the wire underwent a second elongation of ~0.4% during the orthorhombic-to-monoclinic transformation. For each of the subsequent  $M_S$  tests in Figures 2c through 2e the load was removed at an earlier stage of the first transformation. Once the load is removed, no additional strain is realized during the remainder of the first transformation. Although a strain is observed during the second transformation, in each case it is correspondingly reduced. The test in Figure 2e had the load removed immediately after the onset of the initial cubic-to-orthorhombic transformation. Still a small second elongation occurred during the second (orthorhombic-to-monoclinic) transformation.

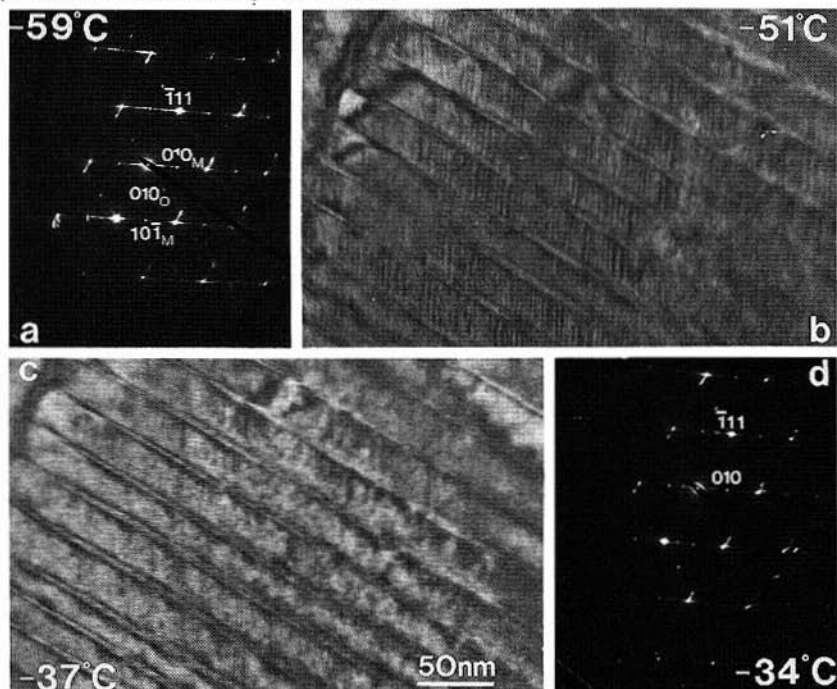


Figure 1: a) [101] zone axis SAD pattern acquired at  $-59^{\circ}\text{C}$ , exhibiting (010) twinned monoclinic martensite within some of the (111) orthorhombic twins. Streaking is due to the fine spacing of the (010) twins. b) BF image acquired at  $-51^{\circ}\text{C}$ , exhibiting fine monoclinic twins ~3-4 nm in width. c) BF image acquired at  $-37^{\circ}\text{C}$  which exhibits the fine twins as disappearing. d) [101] zone axis SAD pattern acquired at  $-34^{\circ}\text{C}$  exhibiting less streaking in conjunction with the removal of the (010) monoclinic twin planes.

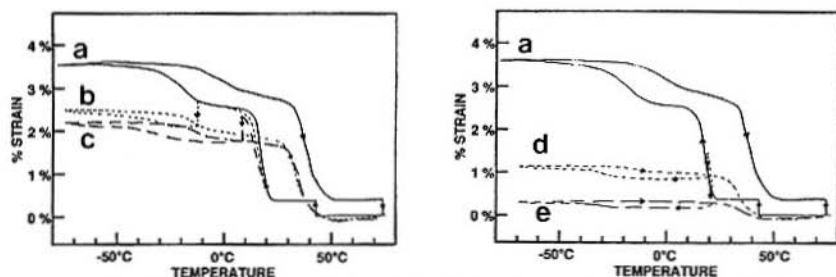


Figure 2: a) Solid line represents  $M_S$  test for strain vs temperature, with a load of 60 MPa applied throughout the entire transformation, both cooling and heating. b) through e)  $M_S$  tests where load is removed during the first transformation at progressively higher temperatures.

## DISCUSSION

The two-step martensitic transformation, from cubic to orthorhombic to monoclinic upon cooling, in TiNi(10% Cu) shape memory alloys was confirmed in this study. Although various twin systems are possible for both cubic-to-monoclinic transformations (with  $\{111\}$ ,  $\{010\}$  and  $\{011\}$  twin planes) and cubic-to-orthorhombic transformations (with  $\{011\}$  and  $\{111\}$  twin planes), the crystallographic similarities of these two transformations require the orthorhombic-to-monoclinic transformation to occur via the incorporation of  $\{010\}$  monoclinic twins. The distortions incurred in each step of the two-step transformation can be visualized by the schematic two-dimensional unit cells exhibited in Figure 3 (see below). Upon cooling, the  $\{011\}$  projection of the B2 cubic cell transforms to a  $\{001\}$  projection of the B19 orthorhombic cell, which then transforms to the  $\{001\}$  projection of the B19' monoclinic cell. The two steps of an ideal transformation, where a single crystal of cubic structure transforms to a 'twinless' orthorhombic structure and then transforms to  $\{010\}$  twinned monoclinic martensite, result in longitudinal distortions of 5.7% strain and 1.8% strain, respectively. The relative ratio of these two longitudinal distortions is 0.32, yet a larger ratio would be realized if the elongation occurs at an angle closer to the diagonal of the unit cells. If a single crystal of the cubic structure transforms to  $\{111\}$  twinned orthorhombic martensite and then to  $\{010\}$  monoclinic twins within the orthorhombic twins, the relative ratio of strains increases to 0.35 [2, 17]. When the  $\{011\}$  twinned orthorhombic martensite forms first, the relative ratio increases to 0.43. The wire used in these tests is polycrystalline and causes the elongations achieved to be less than ideal. However, the relative ratio of experimental strains is related to that of the calculated strains.

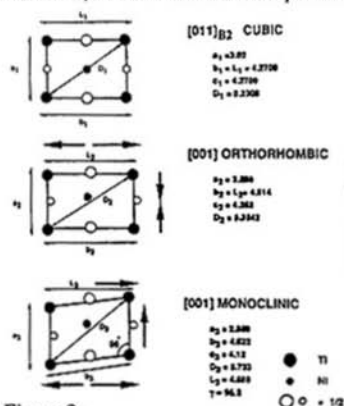


Figure 3:

## EXPERIMENTAL STRAINS

ELASTIC STRAIN	STRAIN RECOVERED WHEN LOAD REMOVED	B2 - B19 CUBIC TO ORTHORH.	B19 - B19' ORTHORH. TO MONOCLINIC	STRAIN RATIO		
	60 MPa Load During Test	-0.4%	2.25%	1%	0.44	
	Load Removed During Test	-0.4%	-0.6% (of which -0.4% is elastic)	2%	0.4%	0.2
		-0.6%	1.8%	0.4%	0.23	
		-0.6%	0.9%	0.25%	0.29	
		-0.6%	0.35%	0.15%	0.43	

TABLE I

The  $M_s$  tests with the load removed during the transformation determine the two stages of the shape change to be interdependent. The various strains (elastic, pseudoelastic, and recovered) incurred for the different  $M_s$  tests of Figure 2 are presented in Table I. In addition, the ratio of the two strains incurred in the two stages of the transformation are listed. This ratio is shown to be highest (0.43) for the case where the load is removed just after the onset of the first transformation (Figure 2e). This ratio is comparable to that of the ideal case for (011) twinning in the orthorhombic martensite. (The (011) twinning was shown by TEM to be predominant in the orthorhombic martensite.) Since the wire is polycrystalline, the first grains to transform would be those with a preferred orientation for elongating the wire as the transformation to orthorhombic martensite is stress induced. These same grains would also expect to undergo the greatest relative strain when subsequently transforming to monoclinic martensite. Grains of austenite with less preferred orientations are transformed to martensite at a lower temperature of the first transformation, and would consequently provide less additional (relative) strain during the second transformation.

## CONCLUSION

$Ti_{50}Ni_{(50-x)}Cu_x$  shape memory alloys not only exhibit a more narrow hysteresis between heating and cooling transformations, but alloys with ~10% Cu also exhibit a two-step shape change corresponding to a two-step martensitic transformation. *In situ* TEM heating and cooling experiments show the crystallographic relationships between the orthorhombic and monoclinic martensite phases require the second step of the martensitic transformation to occur via the formation of (010) twins in the monoclinic martensite. Strain vs temperature  $M_s$  tests, where the applied load is removed during the first step of the transformation, determine the two successive shape changes are interdependent. Correlating the crystallographic analysis of the TEM with the shape change tests indicate how the second shape change will always be in a direction related to (and in proportion to) the first step's shape change.

## REFERENCES

1. W.J. Moberly and K.N. Melton, in Engineering Aspects of Shape Memory Alloys, (ed. by T.W.Duerig and C.M.Wayman), Butterworths, London (1990).
2. W.J. Moberly, PhD Thesis: "Mechanical Twinning and Twinless Martensite in Ternary TiNi Alloys", Stanford University, (1991).
3. O. Mercier, K.N. Melton, R. Gotthardt and A. Kulik, Proc. Int. Conf. on Solid-Solid Phase Transformations, (ed. H.L. Aaronson, D.L. Laughlin, R.F. Sekeika, and C.M. Wayman, p1259-63 (1982).
4. O. Mercier, & K.N. Melton, Met Trans., V10A, p387-389 (1979).
5. R.H. Bricknell, K.N. Melton and O. Mercier, Met Trans. V10A, p693-697 (1979).
6. T. Tadaki and C.M. Wayman, Metallography, V15, p233-258 (1982).
7. V. Y. Yerofeyev, L.A. Monasevich, V.A. Pavskaya and Y.I. Paskal, Phys. Metals V4 (1), p86-92 (1982).
8. W.J. Moberly, J.L. Proft, T.W. Duerig & R. Sinclair, ICOMAT 89, (ed. by B.C. Muddle) Trans. Tech. Publications Ltd., p605-611 (1990).
9. S.P. Alisova, N.V. Volynskaya, P.B. Budberg & A.N. Kobylkin, Izvestiya Akademii Nauk. SSSR. Metall., V5, p210-212 (1986).
10. G.M. Michal & R. Sinclair, Acta Cryst., V37B, p1803-1807 (1981).
11. S.P. Gupta and A.A. Johnson, Trans. JIM, V14, p292 (1973).
12. K.M. Knowles, and D.A. Smith, Acta Metall., V29, p101 (1981).
13. R. Sinclair, AIP Conf. Proc., V53, p269 (1979).
14. G.M. Michal, PhD Thesis: "Diffusionless Transformations in TiNi", Stanford University (1979).
15. G.B. Olson & M. Cohen, Met. Trans., V7A, p1897-1923 (1976).
16. Otsuka, K. & K. Shimizu, "Stress-Induce Martensitic Transformations and Martensite-to-Martensite Transformations." Proc. Int. Conf. on Solid-Solid Phase Transformations, (H.L. Aaronson, D.L. Laughlin, R.F. Sekeika & C.M. Wayman, eds.), Pittsburg, p.1267-1286 (1982).
17. W.J. Moberly, T.W. Duerig & R. Sinclair, to be published in Scripta Met.
18. W.J. Moberly & R. Sinclair, to be published.